I&EC research
Industrial & Engineering Chemistry Research

Article

pubs.acs.org/IECR

Study on β-Nucleated Controlled-Rheological Polypropylene Random Copolymer: Crystallization Behavior and a Possible Degradation Mechanism

Jiashu Fan and Jiachun Feng*

State Key Laboratory of Molecular Engineering of Polymers, Department of Macromolecular Science and Laboratory of Advanced Materials, Fudan University, Shanghai 200433, People's Republic of China

Supporting Information

ABSTRACT: Controlled-rheological polypropylene random copolymer (CRPPR) and β-nucleated CRPPR were prepared through peroxide-initiated reactive extrusion and their crystallization behaviors were comparatively investigated. Rheological experiments indicated that all degraded samples acquired better flow properties than undegraded samples and the addition of β-nucleating agent has little effect on the flowability. Unlike conventional controlled-rheological polypropylene homopolymer of which the shortened molecular chains are unfavorable for β-nucleation, the structure characterizations in this work demonstrated an unexpected increase in the β-phase content of degraded β-nucleated CRPPRs with elevated peroxide concentration. Successive self-nucleation and annealing thermal analysis revealed the generation of thicker lamellar in highly degraded samples, which implied that the stereo regularity improved when the molecular chain reacted with peroxide. Based on the experimental results, a possible degradation mechanism was proposed that free radicals preferentially attack the tertiary carbon atoms adjacent to ethylene co-units during the degradation reaction, which resulted in a reduction of stereo errors, and, consequently, improvement of the β-crystallization ability.

INTRODUCTION

Isotactic polypropylene (iPP) is showing rapid industrial development, because of its low cost and versatile applications. However, commonly used homopolymerized polypropylene (PPH) is primarily limited in some industrial applications, because of its poor impact resistance, especially at low temperatures. Copolymerization with ethylene and other olefins is one of the effective ways to overcome this shortcoming.[1−3] Various types of polypropylene (PP) copolymers can be produced by means of copolymerization, among which polypropylene random copolymer (PPR) stands out for its excellent mechanical properties.[4−6] In this copolymer, ethylene co-units are randomly embedded in the main chain, which disrupts the crystallization of the propylene sequence and thus leads to a decrease in melting temperature and crystallinity.[7,8] As a result, PPR acquires superior toughness and moderate strength, which makes it a widely used matrix component in pipe, automobile parts, furniture, and other industrial uses. Besides copolymerization, optimizing the crystalline structure of PP is also a feasible way to improve its toughness. It is well-known that PP chains can organize into different spatial arrangements, giving rise to several crystalline polymorphs: monoclinic α-form, trigonal β-form, orthorhombic γ-form, and mesomorphic smectic form.[9] The β-nucleated PP has better impact resistance, in comparison with PP in other forms.[10−15] The general beliefs have been that the improved impact resistance of β-PP origins from the intrinsic crystalline structure and the stress-induced transformation from a less-dense crystalline structure (β-phase) to a more-dense crystalline structure (α-phase).[16] Therefore, further improving the toughness of PPR by means of β-nucleation may be an effective way to produce supertoughened PP products.

In some industrial applications, such as high-speed spinning and injection-molded thin-walled production, the PP used requires not only high impact resistance but also excellent melt flow properties. However, commercial PP polymerized by conventional Ziegler−Natta catalyst systems usually has a high molecular weight (MW) and a broad molecular weight distribution (MWD), which lead to its high melt viscosity and elasticity.[17−19] To improve the processability and achieve the diversity in the applications of polypropylene, a "controlled-rheology polypropylene" (CRPP) technology was developed and widely adopted.[20−26] This technology is carried out in reactive extrusion operations using peroxide-initiated scission reactions. With a combined action of shear, temperature, and the addition of organic peroxide in a post-reactor procedure, CRPP can be produced through a β-scission reaction of original PP which statistically favors the rupture of the highest-MW chains first.[20−26] Because of the decreased MW and narrower MWD, CRPP possesses many properties that are superior to normal PP, such as much higher melt flow rate (MFR), less shear sensitivity, better transparency, and surface smoothness, which widely broadens the application potentials of PP. However, it is reported that the impact resistance of CRPP is even worse, because of the decreased MW,[21,22] which limits its further applications.

Transforming the crystalline form of CRPP from α to β may be an efficient way to simultaneously improve its toughness and processability.[27] Considering the intrinsic high impact resist-

Received: September 13, 2012
Revised: December 12, 2012
Accepted: December 14, 2012
Published: December 14, 2012

dx.doi.org/10.1021/ie302474b | Ind. Eng. Chem. Res. 2013, 52, 761−770

ance of PPR, it is possible to achieve products with both excellent toughness and processing flowability by preparing β-nucleated controlled-rheological polypropylene random copolymer (CRPPR). Surprisingly, to our knowledge, there are very few works in the open literature that have addressed the combination of the β-nucleation with CRPPR. In the only study of β-nucleated CRPPR, Cao et al. reported that, at relatively low peroxide concentrations, the β-phase content of β-nucleated CRPPR decreased slightly compared to that of β-nucleated parent PPR, and the mechanical properties showed no significant changes with peroxide content.[28] However, the detailed chemistry mechanism including whether and how the occasional insertion of ethylene co-units would affect the degradation of PPR, as well as physical mechanism including how the change in macromolecular structure would affect the crystallization behavior, especially the formation of β-modification, are far away from a complete understanding.

In previous studies, it has already been shown that the crystallization behavior of β-PP is greatly dependent on its molecular structure.[11−13,29] Busse et al. demonstrated that the insertion of ethylene comonomer, which greatly affected the stereoregularity of the molecular chain, decreased the ability to generate β-crystalline and the β-phase content decreased with increasing ethylene comonomer content.[29] Varga et al. suggested that copolymerization of ethylene into PP slowed the development of the β-phase, and this was ascribed to the lower growth rate of the β-phase with increasing ethylene content.[11] Not only the variation of stereoregularity but also the change in molecular weight would have remarkable influences on the crystallization behavior of β-PP. Varga and his co-workers also reported that the formation of β-form was much easier in higher-MW PP,[11,13] which was further confirmed by other groups.[12,30,31] Thus, in β-nucleated CRPPR, the decreased MW and the randomly inserted ethylene co-units will certainly have prominent impacts on its crystallization behavior as well. In return, the investigation of crystallization behavior of β-nucleated CRPPR will also provide fundamental insight into degradation process of PPR and therefore be meaningful for the production of high-performance PP-based materials in the industrial field.

In this work, we carried out a comparative study on the crystalline behavior of a common CRPPR and β-nucleated CRPPRs. The variation in β-phase content with increasing peroxide concentration had been paid much attention and special emphasis is placed upon the influence of degradation reaction on the crystallization behavior of β-nucleated CRPPR. Based on our results, a possible degradation mechanism of PPR was also proposed.

EXPERIMENTAL SECTION

The material under study was a PPR with a melt flow rate of 2.2 g/10 min (230 °C/2.16 kg), M_w of 5 × 10^4 g/mol, M_w/M_n of 5.2 and an ethylene content of 3.4 wt %, supplied by Yanshan Petrochemical Co., SINOPEC (Beijing, China). Dicumyl peroxide (DCP) was obtained from Shanghai Reagent Corporation (Shanghai, China). The β-nucleating agent (β-NA) was aryl amide compounds (TMB-5), which was supplied by Shanxi Institute of Chemical Industry (Taiyuan City, China). The chemical structures of the chemicals and polymers used are presented in Scheme 1.

The β-nucleated CRPPR samples were prepared in a two-step procedure: first, PPR was mixed with 0.1 wt % β-NA and various amounts of DCP in a high-speed mixer for 5 min;

Scheme 1. The Chemical Structures of (A) DCP, (B) TMB5, and (C) PPR

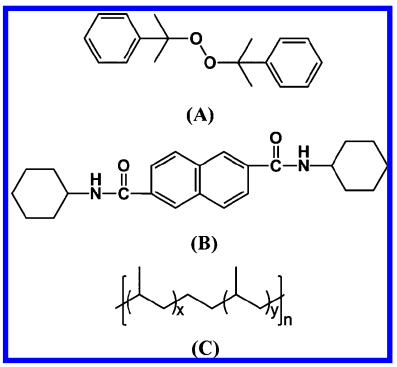

second, the mixture was extruded in a SJ-20Z/25 single-screw extruder with a temperature profile of 180−220 °C and then pelletized and dried. The resulting pellets with DCP contents of 0, 0.1, 0.2, 0.3, 0.4, 0.5, and 0.6 wt % were marked as β-CRPPR-0, β-CRPPR-1, β-CRPPR-2, β-CRPPR-3, β-CRPPR-4, β-CRPPR-5 and β-CRPPR-6, respectively. For comparative purpose, the pellets without β-NA were also prepared in an identical procedure. The resulting pellets with DCP contents of 0, 0.1, 0.2, 0.3, 0.4, 0.5, and 0.6 wt % were marked as CRPPR-0, CRPPR-1, CRPPR-2, CRPPR-3, CRPPR-4, CRPPR-5 and CRPPR-6, respectively. Specially, CRPPR-0 and β-CRPPR-0 are samples produced without adding of DCP and used as undegraded references.

The pellets of all samples were molded to sheets and bars for mechanical tests. The dog-bone specimens used for tensile testing, with dimensions of 20 mm × 4 mm × 0.5 mm, were cut from the molded 0.5-mm-thick sheets. The tensile testing was conducted on a SANS CMT-6503 universal testing machine (Shenzhen, PRC) with a crosshead speed of 50 mm/min. The bars, with a size of 100 mm × 10 mm × 4 mm are used for Izod impact tests after notches were machined (notch depth = 2.0 ± 0.1 mm). Notched impact tests were carried out using an XJJ impact tester (Changchun, PRC), following ASTM Standard Method D256-04. The maximum impact energy of pendulum is 0.98 J. All specimens were conditioned at a temperature of 22 ± 0.5 °C for 12 h before testing. These values were measured under the same conditions and each reported mechanical result is an average value of at least six measurements.

Melt flow rate (MFR) was measured following ASTM D 1238 using a XNR-400B MFR tester (Changchun, PRC) at 230 °C/2.16 kg. An Advanced Rheometric Expansion System (ARES) rheometer with torsional parallel plate geometry, in combination with a temperature-controlled oven, is used to test the rheological properties in this study. Samples for rheological measurements were compression-molded to form 25-mm disks at 200 °C, using a laboratory mixing molder (LMM). The torque and strain resolution is 1 nN m and 0.04 μrad, respectively, and the accuracy of temperature-controlled oven is ±0.1 °C. The dynamic measurements are carried out in the linear domain for frequencies ranging from 0.1 rad/s to 100 rad/s at 190 °C in nitrogen.

Wide-angle X-ray diffraction (WAXD) measurements were carried on a PANalytical X'pert diffractometer (PANalytical, The Netherlands) in a reflection mode using Ni-filtered Cu Kα radiation (λ = 0.154 nm) under a voltage of 40 kV and a current of 40 mA. Intensity versus diffraction angle 2θ was recorded in the region from 10° to 30°. Subsequently, following

dx.doi.org/10.1021/ie302474b | Ind. Eng. Chem. Res. 2013, 52, 761−770

Hsiao's method of analyzing WAXD data, the overall crystallinity (X_c) was determined using the following equation by deconvoluting the peaks in linear WAXD profiles:

$$X_c\ (\%) = \frac{A_c}{A_c + A_a} \times 100 \quad (1)$$

where A_c and A_a are the areas of crystalline peaks and amorphous halo, respectively.[32] The relative content of the β-crystals (K_β) then was evaluated by the method that Turner-Jones et al.[33] proposed:

$$K_\beta = \frac{H_\beta(300)}{H_\beta(300) + H_\alpha(110) + H_\alpha(040) + H_\alpha(130)} \quad (2)$$

where $H_\beta(300)$ is the height of the (300) reflection peak; $H_\alpha(110)$, $H_\alpha(040)$, and $H_\alpha(130)$ are the height of the (110), (040), and (130) reflection peaks, respectively.

The thermal properties were measured using a differential scanning calorimetry (DSC) 821e thermal analysis system (Mettler Toledo Instruments Inc., Switzerland). Calibration for the temperature scale was performed using indium (T_m = 156.60 °C and ΔH_m^0 = 28.45 J/g) as a standard, to ensure reliability of the data obtained. The accuracy of measured temperature is ±0.05 °C. All the experiments were carried out in a nitrogen atmosphere. For regular melting and crystallization analysis, the measurements were performed as following procedures: samples were heated to 200 °C and kept for 5 min to erase previous thermal history. Subsequently, samples were cooled to 25 °C at a rate of 10 °C/min, and again heated to 200 °C at a rate of 10 °C/min. The crystallization thermograms were recorded during the first cooling scan, while the melting temperature and fusion enthalpy of the samples were determined during the second heating scan.

DSC is also used to estimate the relative content of the β-form and the overall crystallinity to compare with those calculated from WAXD data. The relative content of β-form estimated by DSC melting curves may be defined as ϕ_β and calculated from the following equation:

$$\varphi_\beta\ (\%) = \frac{X_\beta}{X_\alpha + X_\beta} \times 100 \quad (3)$$

where X_α and X_β are the crystallinity of the α- and β-form, respectively, and could be calculated separately, according to

$$X_i\ (\%) = \frac{\Delta H_i}{\Delta H_i^0} \times 100 \quad (4)$$

where ΔH_i and ΔH_i^0 are the calibrated specific fusion heat and the standard fusion heat of either α- or β-form, respectively. The values of ΔH_i^0 used in our work are 177 J/g for α-form and 168.5 J/g for β-form.[34] Because of the coexistence of α- and β-forms, the samples exhibited both an α- and a β-fusion peak on DSC curves, which overlapped partially. The total fusion heat was estimated by integrating the DSC thermogram from 60 °C to 160 °C. A vertical line was drawn through the minimum between the α-fusion peak and β-fusion peaks, and the total fusion heat was divided into β-component and α-component. The specific fusion heats for α- and β-forms were determined according to the calibration method reported in refs 35−37.

The successive self-nucleation and annealing thermal analysis (SSA) used for the thermal fractionation of CRPPR samples involved a series of heating−annealing−cooling cycles and was performed according to the following procedures: samples were first heated to 200 °C at 10 °C/min and kept for 5 min, then cooling to 25 °C at 10 °C/min to create an initial "standard" thermal history. Secondly, samples were heated to a selected self-seeding temperature (T_s) at 10 °C/min and maintained at this temperature for 5 min. This step results in partial melting and annealing of unmelted crystals, while some of the melted species may isothermally crystallize. Crystallization after self-nucleation was achieved by subsequently cooling samples to 25 °C at 10 °C/min. After a series of thermal fractionation processes, samples were finally heated from 25 °C to 200 °C at 10 °C/min and the corresponding endothermic curves were recorded. Because CRPPR-0 was the reference sample in our work, we chose the ideal first T_s value of CRPPR-0 as the first T_s value to perform SSA experiments for all samples. Following Muller's method,[38] we selected 149 °C as the first T_s value in our SSA procedure after a series of self-nucleation experiments (see the Supporting Information). The fraction window adopted here was 5 °C, and the annealing time was 5 min. The temperature range for thermal fractionation was from 149 °C to 99 °C at an interval of 5 °C for CRPPR samples. The scanning rate used during the thermal conditioning steps was 10 °C/min.

RESULTS AND DISCUSSION

Rheological Properties. Figure 1 shows the MFR values of the samples prepared with various peroxide concentrations.

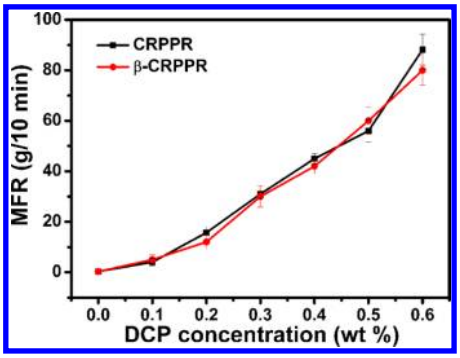

Figure 1. MFR values of non-nucleated and β-nucleated samples prepared with various DCP concentrations.

The MFR of both non-nucleated and β-nucleated samples increases noticeably with the increase of DCP content, and no evident difference can be detected between CRPPRs and its β-nucleated counterparts. MFR results suggest that the DCP-induced degradation reaction decreases the molecular weight of PPR and the addition of β-NA has little effect on the MFR of CRPPRs. Moreover, it can be seen from Figure 1 that the MFR values increase almost linearly with DCP concentration, and the extent of the increase is comparable to that of CRPPH reported in previous work.[26] As mentioned above, the difference of molecular structure between PPR and PPH is the random insertion of ethylene comonomers in propylene sequence. When PPH molecular chains react with free radicals, hydrogen abstraction from PPH backbones proceeds preferably at the site of the tertiary carbon atom, which leads to the β-fragmentation reaction of tertiary alkyl radicals.[21,22,25] As for copolymerized PP, studies on controlled-rheological block copolymerized polypropylene (PPB) indicate that PP matrix degrades while the long ethylene sequence tends to branch and cross-link by macroradical recombination, which results in the presence of

dx.doi.org/10.1021/ie302474b | Ind. Eng. Chem. Res. 2013, 52, 761−770

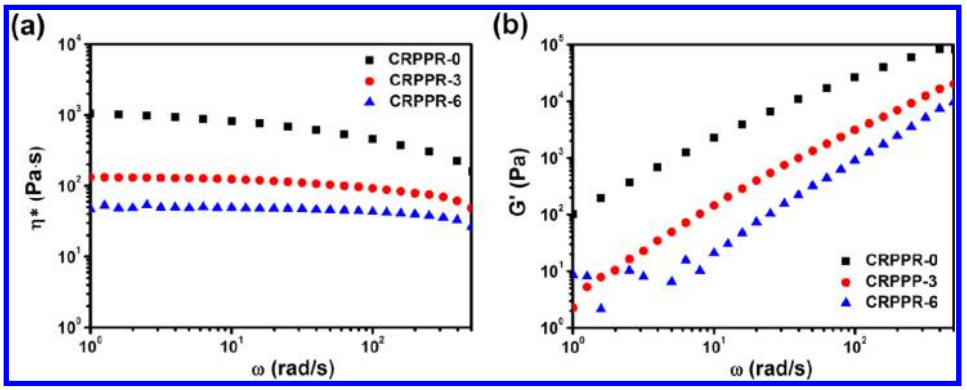

Figure 2. Evolution of (a) complex viscosity and (b) storage modulus with frequency for three CRPPRs.

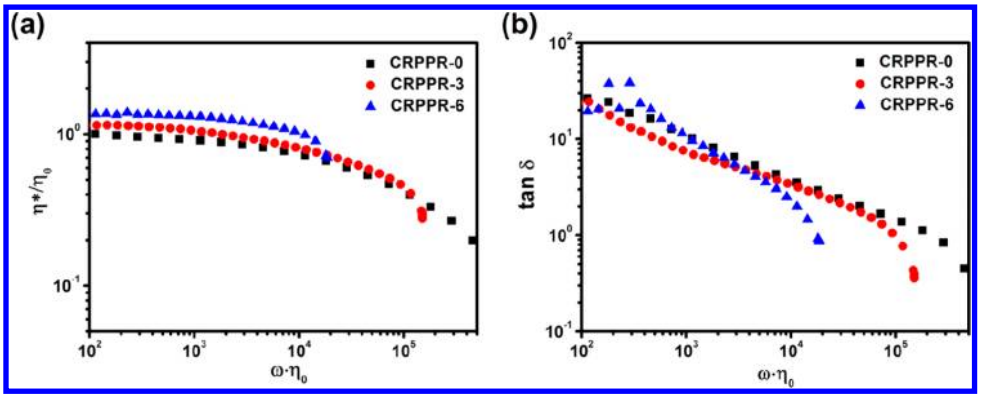

Figure 3. Variation of (a) η^*/η_0 and (b) tan δ with $\omega\eta_0$ for three CRPPRs.

high residual masses and much less increased MFR, compared to that of CRPPH.[25,26] Thus, the similar MFR results of CRPPR and CRPPH might suggest that there are almost no branching or cross-linking reactions in our experiment.

The complex viscosity (η^*) and storage modulus (G') of three CRPPRs prepared with different DCP concentrations (0, 3, and 0.6 wt %) measured by ARES are displayed in Figure 2. As obvious from Figure 2a, degraded CRPPRs have much lower η^* values than the undegraded one. The dependence of complex viscosity on DCP concentration indicates the decreasing molecular weight of PPR with elevated DCP concentration, which is in accordance with the trend of the variation of MFR. Furthermore, the decline of η^* values with increasing frequency for CRPPRs is much slower than that for the reference CRPPR-0. The less-pronounced shear-thinning effects of the products can be explained by the decrease of the chain entanglement density, which is caused by the DCP-induced break of molecular chains. As G' greatly depends on the molecular weight, the G' values of CRPPRs also decrease with increasing DCP concentration (Figure 2b), indicating that the degraded products are less elastic than the undegraded ones.

The variation of η^*/η_0 and tan δ with $\omega\eta_0$ for three CRPPRs prepared using different DCP concentrations are shown in Figure 3, from which we can drawn the information of the change of MWD caused by degradation.[39] ω is the frequency used in dynamic frequency measurements, ranging from 0.1 to 100 rad/s. η_0 is the viscosity measured at zero shear rate and the η_0 values of CRPPR-0, CRPPR-3, CRPPR-6 are 1047.7, 132.9, 41.1 Pa s, respectively. Wood-Adams's work on the effect of molecular structure on the linear viscoelastic behavior of polyethylene has demonstrated that the transition zone between the Newtonian plateau and the high-frequency power law zone broadens when broadening the MWD.[39] Similarly, we can see from Figure 3a that this transition zone narrows with DCP concentration increasing from 0 to 0.6 wt %. Figure 3b also shows the narrowing effect in the loss angle. Both Figure 3a and Figure 3b can provide evidence for the narrowing MWD of the polymer caused by the degradation of high-MW molecule tails in PPR chains.[39]

Fracture and Tensile Behavior. The evolution of Notched Izod impact strength for non-nucleated and β-nucleated samples prepared with various DCP concentrations is exemplified in Figure 4. As expected, with the addition of 0.1 wt % β-NA, the impact strength of PPR greatly improves from 12.3 kJ/m^2 for CRPPR-0 to 15.6 kJ/m^2 for β-CRPPR-0. The β-NA-induced formation of β-phase is believed to be the reason

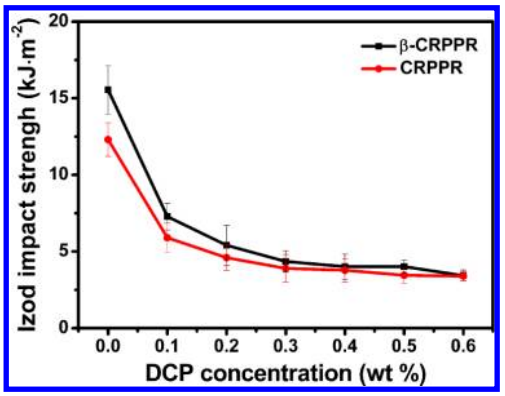

Figure 4. Notched Izod impact strength of non-nucleated and β-nucleated samples prepared with various DCP concentrations.

dx.doi.org/10.1021/ie302474b | Ind. Eng. Chem. Res. 2013, 52, 761−770

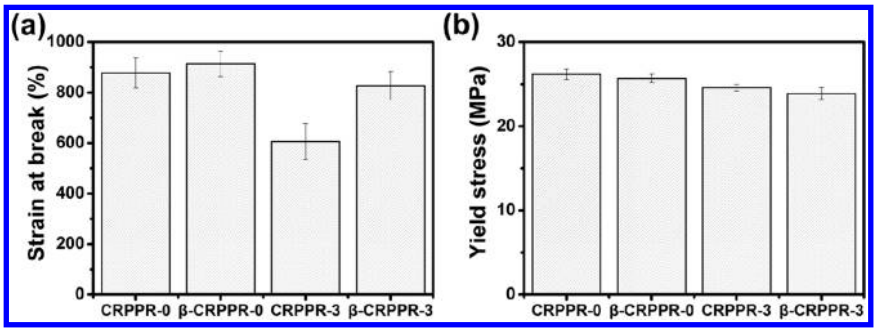

Figure 5. (a) Strain at break and (b) yield stress of four samples.

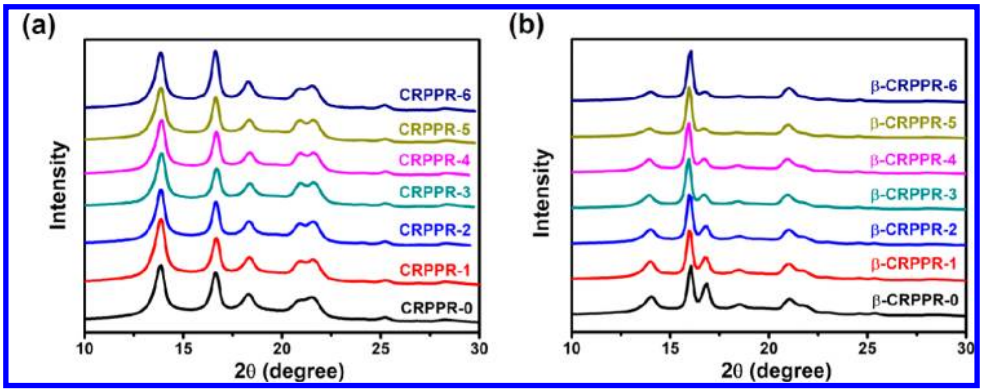

Figure 6. WAXD diffraction patterns of (a) non-nucleated and (b) β-nucleated samples.

for the enhancement in impact strength. Compared to the undegraded reference sample β-CRPPR-0, this improvement becomes less pronounced for degraded β-CRPPRs and even undetectable for the sample with 0.6 wt % DCP. Although the impact strength of degraded β-CRPPRs is much lower than that of β-CRPPR-0, it is generally higher than that of CRPPR at the same DCP concentration, which can be partly ascribed to the excellent impact property of β-nucleated PP.

The tensile strain at break and yield stress obtained from stress−strain curves are showed in Figure 5. Only the results of CRPPR-0, CRPPR-3, β-CRPPR-0, and β-CRPPR-3 are taken to make a simple comparison. As can be seen from Figure 5a, the strain at break of CRPPR decreases with the amount of 0.3 wt % DCP but improves largely with the addition of 0.1 wt % β-NA. The specific increase in the strain at break of CRPPR when transforming the crystalline form of CRPPR from α to β indicates a significant enhancement in toughness, which is in accordance with the result of impact tests. Figure 5b shows that the yield stress decreases slightly with the introduction of β-NA. This may be attributed to the looser lamellar structure of β-crystal with respect to that of α-crystal. With the addition of 0.3 wt % DCP, a slight decrease is observed in the yield stress of both PPR and β-PPR, which can be ascribed to the decreased molecular weight. The results of both impact and tensile tests have revealed that the reduced mechanical properties of CRPPR, which result from the DCP-induced lower entanglement density, can be improved by transforming the crystallographic phases from α to β. It is generally accepted that β-phase acquires better toughness and lower strength compared to α-phase. The higher tensile strength of α-phase results from the presence of an interlocking effect of the radial lamellae by the tangential crystallites in α-nucleated CRPPR, which also leads to inferior fracture resistance.[15,40] The better toughness of β-nucleated CRPPR is believed to be caused by a stress-induced transformation from a less-dense crystalline structure (β-phase) to a more-dense crystalline structure (α-phase) and better energy dissipation in the absence of a cross-hatched structure.[16,41,42]

Crystalline Structure. The mechanical properties of semicrystalline polymers greatly depend on their crystalline structure and thus, the crystalline structures of the various controlled-rheological samples were investigated. Figure 6a and 6b show the WAXD patterns of non-nucleated and β-nucleated samples, respectively. As is obvious from Figure 6a, no significant difference can be detected among the diffraction patterns of undegraded CRPPR-0 and degraded CRPPRs, which means the crystalline form of samples without β-NA remains unchanged when extruded with organic peroxide. In contrast, one can observe clearly in Figure 6b that all samples with β-NA exhibit the characteristic diffraction peak at 2θ = 16.0°, corresponding to the (300) crystal plane of β-phase. Furthermore, the relative intensity of the (300) peak gets higher with increasing DCP amount, which reflects an increasing content of β-form.

The relative content of β-phase (K_β value) with the increase of DCP concentration is displayed in Figure 7. It is shown that the introduction of 0.1 wt % β-NA induces a β-form content of 53% in CRPPR-0, which is much lower than that of β-nucleated PPH. Previous works[11−13,29] have revealed that the much lower β-phase content of β-CRPPR-0 results from the decreased regularity of the molecular structure, which is caused by the random insertion of ethylene co-units. Generally, β-phase is easier to form in high-MW PP and the decreased MW is unfavorable for the formation of β-phase.[30,31] A study dealing with the influence of MWD on the formation of β-phase also reveals that PP with a narrow polydispersity exhibits a weak ability to form β-phase.[43] Because of the vis-breaking of the molecular chains, CRPP possesses lower MW and narrower

dx.doi.org/10.1021/ie302474b | Ind. Eng. Chem. Res. 2013, 52, 761−770

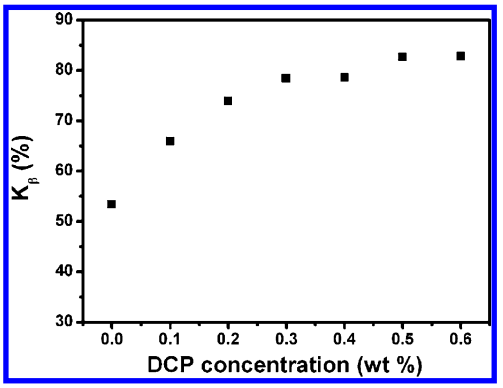

Figure 7. β-phase content of samples prepared with various DCP concentrations.

MWD, which is not advantageous for the formation of β-phase. However, to our surprise, the K_β value of CRPPR in our experiment evidently increases as the DCP concentration increases. With the addition of only 0.1 wt % DCP, the K_β value exhibits a significant increase, from 53% to 66%. When the DCP concentration increased to 0.5 wt %, the K_β value reaches a maximum of 82%, which is comparable to that of β-nucleated PPH (the reported K_β value of β-PPH ranges from 70%[44] to 90%[34,35]). Figures 8a and 8b show the overall crystallinity calculated from both DSC and WAXD measurements, respectively. We can see from both Figures 8a and 8b that the crystallinity remains almost unchanged with various contents of DCP, and the addition of β-NA also causes no evident changes in crystallinity. For some samples, the values calculated from WAXD data are slightly lower than those from DSC data, which may result from the relatively broad integration range of DSC fusion heat from 60 to 160 °C. The crystallinity results suggest that the elevated K_β value does not result from the variation of crystallinity. Therefore, the enhanced β-crystallization ability of CRPPR might be related to the structural changes of molecular chains, except the lower MW or narrower MWD. Considering Busse's research that the insertion of ethylene comonomers weakens the ability to generate β-crystalline and the β-phase content decreases with increasing ethylene comonomer content,[29] the increase in the β-phase content might indicate that the number of ethylene comonomers randomly inserted in PP backbones decreases during degradation process. Therefore, we speculate that the increase in the β-phase content might means the cleavage of molecular chains mainly occurs adjacent to the ethylene comonomers. This will be further investigated in the following parts.

Figures 9a and 9b show the DSC crystallization curves of CRPPRs and β-nucleated CRPPRs, respectively. It can be observed from Figure 9a that the crystallization peak temperature (T_{cp}) of CRPPR-0 is 99.2 °C. After reacting with different amounts of DCP, the T_{cp} value of CRPPR varies within the range of only 1 °C, which means no significant changes of T_{cp} occur during the degradation process. With the introduction of 0.1 wt % β-NA, the T_{cp} of β-CRPPR-0 rises to 110.8 °C, which is ascribed to the nucleation effect of β-NA. Similarly, T_{cp} of degraded β-nucleated CRPPRs remains at ~111 °C, which is close to that of β-CRPPR-0. Therefore, it can be inferred from the crystallization curves that the degradation process has no evident influence on the crystallization temperature of the samples.

The DSC melting curves of non-nucleated and β-nucleated samples are shown in Figure 10a and 10b, respectively. β-nucleated PPR and CRPPRs exhibit three parts of melting peaks at the range of ~125−140 °C, 140−148 °C and 148−160 °C (corresponding to the β-, α1 and α2-crystals, respectively), indicating the melting of β-phase and α-phase. During heating process, the unstable β-phase tends to melt first and then recrystallize as the α-phase with a more-stable crystalline structure.[45] This may be one of the reasons for the emergence of the melting peak α2 in our β-nucleated CRPPRs. The much lower K_β values of β-PPR and β-CRPPRs calculated from DSC data (K_β values of β-CRPPR-0, β-CRPPR-1, β-CRPPR-2, β-CRPPR-3, β-CRPPR-4, β-CRPPR-5, β-CRPPR-6 are 36.1%, 38.4%, 39.6%, 40.3%, 42.9%, 43%, and 45.8%) than those calculated from WAXD data are also the evidence of the melting recrystallization transition of β-phase during the heating process. Compared to the complex melting behavior of β-nucleated CRPPRs, the melting behavior of CRPPRs shows more direct and detailed information which is related to the structural changes in CRPPRs. Figure 10a shows that the broad α-melting peak of PPR divides into two melting peaks gradually, i.e., α1 with lower melting temperatures and α2 with higher ones. The more interesting phenomenon is that, as DCP concentration increases, α1 shifts to a lower-temperature region and α2 shifts to a higher-temperature region. α2 shifting to higher temperature region manifests that parts of the crystalline components of CRPPRs contain thicker lamellar, which is further proven in our latter SSA experiments. When DCP concentration increases, lamellar thickens gradually. Combining the K_β value result and the melting peak shifting to a higher-temperature region, we might conclude that free radicals

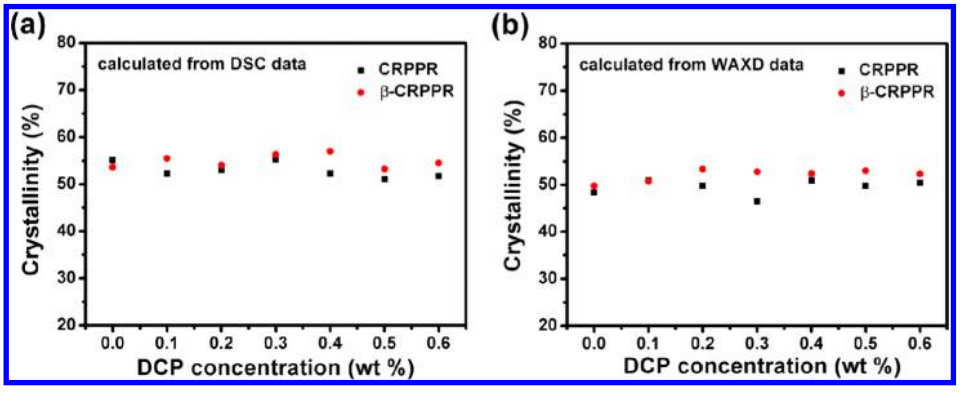

Figure 8. Crystallinity values of non-nucleated and β-nucleated samples calculated from (a) DSC and (b) WAXD data, respectively.

dx.doi.org/10.1021/ie302474b | Ind. Eng. Chem. Res. 2013, 52, 761−770

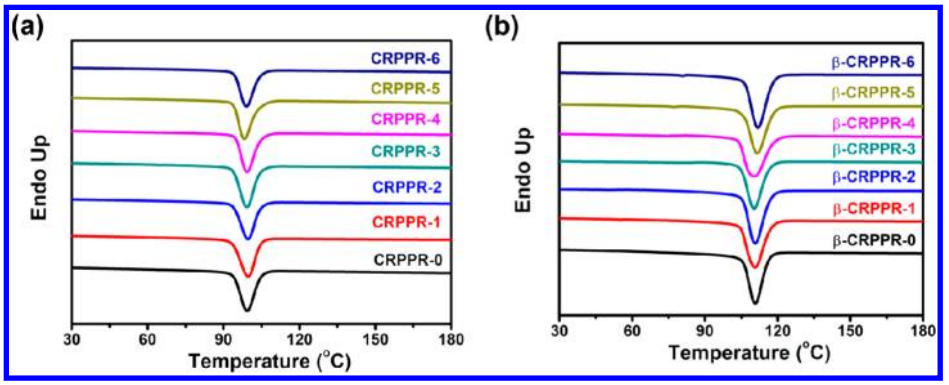

Figure 9. DSC crystallization curves of (a) non-nucleated and (b) β-nucleated samples.

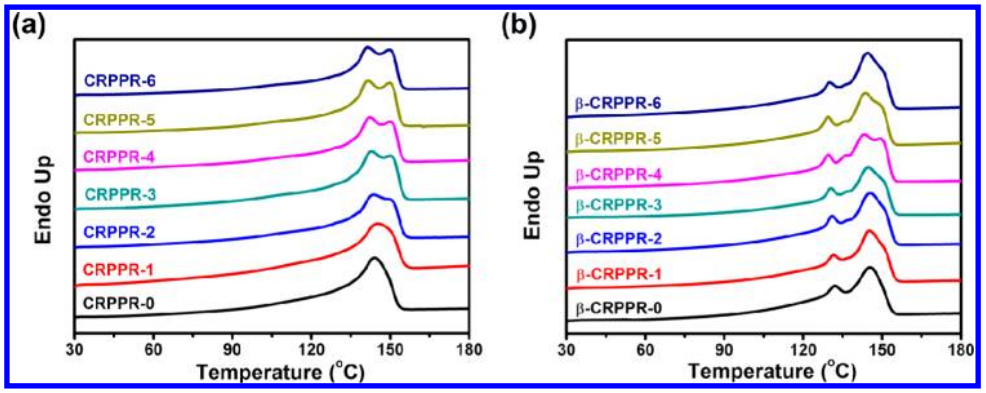

Figure 10. DSC melting curves of (a) non-nucleated and (b) β-nucleated samples.

preferentially attack the tertiary carbons adjacent to the ethylene comonomers. In this way, molecular chains with less stereo defects emerge, which result in the elevated K_β value and the increased melting point of $\alpha 2$. However, during the degradation process, free radicals not only preferentially attack the tertiary carbons adjacent to the ethylene comonomers but they also attack the ordinary ones not close to the ethylene comonomers, especially at high DCP concentration. When the cleavage of molecular chains occurs not close to the ethylene comonomers, the only result of this type of degradation is the decrease in M_w and the number of stereo defects remains unchanged. These components with decreased M_w and unchanged stereo defects are the reason for the decreased melting point of $\alpha 1$ and this melting behavior is in agreement with previous results.[21,27]

To further explore the crystalline structure, SSA fractionation was performed. SSA thermal fractionation enhances the potential molecular fractionation which can occur during crystallization, while encouraging annealing of the unmelted crystals at each stage of the process, so that subtle effects can be magnified. The DSC melting curves of all CRPPRs after SSA fractionation are shown in Figure 11. According to the fractionation temperature, we divide the melting curves into three domains, i.e., Domain I (below 152 °C), Domain II (152−159 °C), and Domain III (above 159 °C). It is evident that all fractionated samples exhibited a series of small melting peaks in Domain I which may correspond to the partially crystalline polypropylene random copolymers. In Domain II, all samples exhibit a strong melting peak at ∼154 °C and no evident difference can be detected among the samples. The peak positions below 159 °C show no evident differences after reactive extrusion, indicating that the degradation reaction did

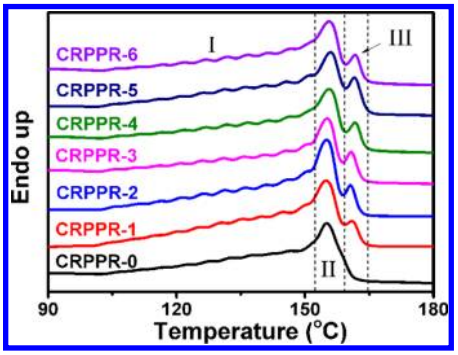

Figure 11. DSC melting curves of CRPPRs after SSA fractionation.

not change the lamellar thickness of these fractionated components. However, the proportion of these components has been changed, as can be seen from the varying resolution of the melting peaks. Surprisingly, in Domain III, it is interesting to see that a new small melting peak emerges at a higher temperature of ∼161 °C. Moreover, by drawing a vertical line through the minimum between Domain II and Domain III, the rough melting fusion heat of the newly emerged melting peak is approximately calculated. The values of CRPPR-0, CRPPR-1, CRPPR-2, CRPPR-3, CRPPR-4, CRPPR-5, CRPPR-6 are 0, 4.52, 5.27, 5.38, 5.86, 7.24, and 7.13 J/g, respectively. The overall trend of the melting fusion heat is, first, to increase with DCP concentration up to 0.5 wt % and then remain at this level. The melting peaks of fractionated samples are related to the melting of crystallites with different lamellar thickness, which are formed at each self-nucleation temperature employed. The higher melting point corresponds to higher lamellar thickness.[45] The newly emerged melting peak above

dx.doi.org/10.1021/ie302474b | Ind. Eng. Chem. Res. 2013, 52, 761−770

159 °C indicates that a new component with the ability to generate thicker lamellar than CRPPR-0 could be fractionated from the degraded CRPPRs and this will help us to make a better understanding of the crystalline structure of CRPPR. During the SSA experiment, the samples at standard state are first heated to the first T_s value (149 °C in our SSA test). Thus, the crystals with melting temperature lower than 149 °C melt and only those with melting temperature higher than 149 °C could survive and act as self-nuclei. Because 149 °C is the ideal first T_s value for CRPPR-0, there is no melting peak in Domain III of CRPPR-0 in Figure 11. However, 149 °C is actually lower than the ideal first T_s value of all degraded CRPPRs and the unmelted crystals will cause annealing of CRPPR during the first self-nucleation step, which, in turn, will generate thicker lamellae and lead to the newly emerged melting peak in Domain III after SSA fractionation. The new melting peak getting stronger reflects that there are an increasing number of crystals whose melting temperature is higher than 149 °C with increasing DCP concentration, which testifies that the amount of lamellae with a high melting point increases as the DCP content increases. As is mentioned above, PPR has a reduced tendency to crystallize, because of the reduced regularity caused by incorporation of comonomer units. Thus, the new component whose melting temperature is close to that of PPH reveals a reduced random insertion of ethylene comonomer units which makes its molecular structure closer to PPH. The improved stereoregularity of CRPPR can also account for the increase in β-crystallinity of β-nucleated CRPPRs.

Although there are few studies focusing on the degradation mechanism of CRPPR, studies dealing with selective functionalization of the ethylene-rich phase of a heterophasic polypropylene might provide some important information for the degradation process. Kamfjord[46] investigated the effect of the solubility parameters of various peroxides on the grafting level of maleic anhydride (MA) in the different phases of a heterophasic polypropylene and found that both the degradation and the functionalization mainly occurred in the ethylene-rich phase. Free radicals preferentially attack single tertiary hydrogens between ethylene units, or at the ends of a PP block, adjacent to one or multiple ethylene units, which results in a selective functionalization of the ethylene-rich copolymers. Schlick's study[47] also suggests heterophasic propylene−ethylene copolymers (HPEC) containing 25% E degrades faster, compared to that containing 10% E, which is determined by the increased rate of oxygen diffusion and reactants mobility in polymers with higher EPR content. Therefore, with our experimental results and the related studies, we may speculate that, during reactive extrusion, the free radicals generated from the decomposition of DCP preferentially attack the tertiary carbon adjacent to ethylene units on the PP backbone and abstract the H atom on it. This will result in polymer chains with ethylene sequence only on the end, which leads to an improvement in the stereoregularity of CRPPR. The component with less stereo errors is the main cause for not only the newly emerged melting peak at high temperatures but also the increasing β-phase content with elevated DCP concentration. The reasons for this special way of degradation may be as follows: first, the H atom of R_3C-H is less stable than that of R_2CH_2 and thus the free radicals tend to attack the tertiary carbons; second, the tertiary sites close to the ethylene comonomers are less stereo-hindered than other tertiary sites, which results in the selective way of degradation. Two possible ways to generate ethylene as end-group from the fragmentation of tertiary alky radical are also exemplified in Scheme 2. One

Scheme 2. Two Possible Ways To Generate Ethylene as an End-Group from the Fragmentation of a Tertiary Alky Radical

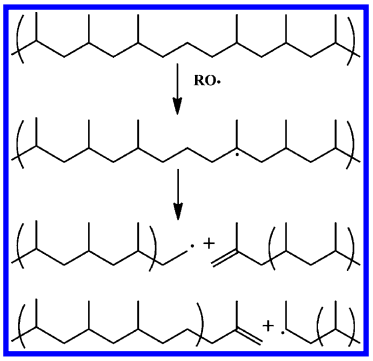

affords terminal olefin with primary alkyl radical and the other affords olefin with secondary alkyl radical. We are prone to the latter one, which is considered to be thermodynamically favored.

A Possible Degradation Mechanism. As discussed above, WAXD tests show that the β-phase content of CRPPR increases with DCP concentration and SSA thermal analysis proves that components with better crystallization ability emerge during the degradation reaction. In accord with these interesting results, we proposed a possible degradation mechanism for the reactive extrusion of CRPPR. As is shown in Scheme 3, the blue ribbon with red plots on it represents the

Scheme 3. Schematic of a Possible Degradation Mechanism

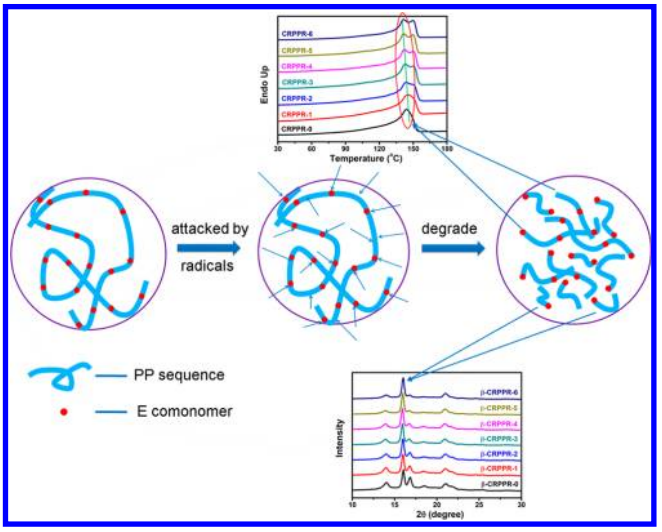

molecular chain of PPR, where the blue ribbon stands for the PP block and the red plots represent the random inserted ethylene comonomer units. When PPR is extruded with organic peroxide at a high temperature, the PPR molecular chains are attacked by free radicals, which are represented by blue arrows in the scheme. It can be seen in the scheme that the free radicals preferentially attack the tertiary carbon adjacent to ethylene units on a PP backbone. As a result, products of the degradation with various structures are achieved. Among the various, polymers with ethylene comonomers in the middle of

dx.doi.org/10.1021/ie302474b | Ind. Eng. Chem. Res. 2013, 52, 761−770

the backbone correspond to the decreased melting points and polymers with ethylene units only on ends of molecular chain and no or few ethylene comonomers in the middle of the backbone account for the newly emerged melting peak above 159 °C in the DSC melting curve after SSA fractionation.

CONCLUSIONS

In this work, both controlled-rheological polypropylene random copolymers (CRPPRs) and β-nucleated CRPPRs were produced using a controlled-rheology method initiated by various amounts of DCP with and without β-NA. When studying the melting and crystallization behavior of the samples, we found that the β-crystallinity of degraded β-nucleated CRPPR unexpectedly increased with elevated DCP content, which is probably attributed to the improvement in stereoregularity of CRPPR. To further investigate the crystalline structure, all CRPPR samples was fractionated by means of SSA, then a new melting peak emerged at temperatures higher than 159 °C, indicating that there exists thicker lamellae in degraded samples. Both the results of the K_β value and the melting behavior analyzed by DSC and SSA testify that the degradation reaction generated a component with an improved stereoregularity. Melt flow rate (MFR) and Advanced Rheometric Expansion System (ARES) tests showed that the mobility of degraded CRPPRs improved as the DCP content increased and the addition of β-NA had no evident influence on the degradation process. The toughness was improved by transforming the crystalline form from α to β. The crystallinity kept almost constant as DCP concentration varied and the addition of β-NA had little effect on it. Combining all our experimental results, a possible degradation mechanism was proposed: during reactive extrusion, free radicals preferentially attack the tertiary carbon atoms adjacent to ethylene monomers and molecular chains with ethylene units only on ends and no or few ethylene comonomers in the middle emerge, and then the stereoregularity of degraded CRPPRs gets improved.

ASSOCIATED CONTENT

Supporting Information

Detailed discussion on the determination of the first T_s value of successive self-nucleation and annealing (SSA) fractionation for the reference sample. This material is available free of charge via the Internet at http://pubs.acs.org.

AUTHOR INFORMATION

Corresponding Author

*Tel.: 86 21 6565 3735. Fax: 86 21 6564 0293. E-mail: jcfeng@fudan.edu.cn.

Author Contributions

The manuscript was written through contributions of all authors. All authors have given approval to the final version of the manuscript.

Notes

The authors declare no competing financial interest.

ACKNOWLEDGMENTS

We gratefully acknowledge the financial support from the Natural Science Foundation of China (Nos. 21174032 and 20874017) National Basic Research Program of China (No. 2011CB605704) and PetroChina Innovation Foundation (No. 2011D-5006-0504).

REFERENCES

(1) Galli, P.; Vecellio, G. Technology: driving force behind innovation and growth of polyolefins. *Prog. Polym. Sci.* **2001**, *26*, 1287−1336.

(2) Poon, B.; Rogunova, M.; Hiltner, A.; Baer, E. Structure and properties of homogeneous copolymers of propylene and 1-hexene. *Macromolecules* **2005**, *38*, 1232−1243.

(3) Rosa, C. de; Auriemma, F.; Ballesteros, O. R. de; Resconi, L.; Camurati, I. Tailoring the physical properties of isotactic polypropylene through incorporation of comonomers and the precise control of stereo and regioregularity by metallocene catalysts. *Chem. Mater.* **2007**, *19*, 5122−5130.

(4) Sanders, J. M.; Komoroski, R. A. A Carbon-13 NMR study of stereochemical configuration in a propylene-ethylene copolymer. *Macromolecules* **1977**, *10*, 1214−1216.

(5) Hosier, I. L.; Alamo, R. G.; Esteso, P.; Isasi, J. R.; Mandelkern, L. Formation of the α and γ polymorphs in random metallocene-propylene copolymers. Effect of concentration and type of comonomer. *Macromolecules* **2003**, *36*, 5623−5636.

(6) Zhang, X.; Shi, G. Effect of converting the crystalline form from α to β on the mechanical properties of ethylene/propylene random and block copolymers. *Polymer* **1994**, *35*, 5067−5072.

(7) Harding, G. W.; Reenen, A. J. van. Fractionation and characterisation of propylene-ethylene random copolymers: effect of the comonomer on crystallisation of poly(propylene) in the γ-Phase. *Macromol. Chem. Phys.* **2006**, *207*, 1680−1690.

(8) Feng, Y.; Hay, J. N. The characterisation of random propylene−ethylene copolymer. *Polymer* **1998**, *39*, 6589−6596.

(9) Varga, J. In *Polypropylene, Structure, Blends, and Composites*; Karger-Kocsis, J., Ed.; Chapman & Hall: London, 1995; Vol. *1*, p 56.

(10) Shi, G.; Chu, F.; Zhou, G.; Han, Z. Plastic deformation and solid-phase transformation in β-phase polypropylene. *Makromol. Chem.* **1989**, *190*, 907−913.

(11) Varga, J. β-modification of isotactic polypropylene: Preparation, structure, processing, properties, and application. *J. Macromol. Sci. Phys.* **2002**, *41*, 1121−1171.

(12) Grein, C. Toughness of neat, rubber modified and filled β-nucleated polypropylene: from fundamentals to applications. *Adv. Polym. Sci.* **2005**, *188*, 43−104.

(13) Chen, H. B.; Karger-Kocsis, J.; Wu, J. S.; Varga, J. Fracture toughness of α- and β-phase polypropylene homopolymers and random- and block-copolymers. *Polymer* **2002**, *43*, 6505−6514.

(14) Grein, C.; Plummer, C. J. G.; Kausch, H.-H.; Germain, Y.; Béguelin, Ph. Influence of β nucleation on the mechanical properties of isotactic polypropylene and rubber modified isotactic polypropylene. *Polymer* **2002**, *43*, 3279−3293.

(15) Tordjeman, Ph.; Robert, C.; Marin, G.; Gerard, P. The effect of α, β crystalline structure on the mechanical properties of polypropylene. *Eur. Phys. J. E* **2001**, *4*, 459−465.

(16) Karger-Kocsis, J. How does "phase transformation toughening" work in semicrystalline polymers? *Polym. Eng. Sci.* **1996**, *36*, 203−210.

(17) Eckstein, A.; Suhm, J.; Friedrich, C.; Maier, R.-D.; Sassmannshausen, J.; Bochmann, M.; Mülhaupt, R. Determination of plateau moduli and entanglement molecular weights of isotactic, syndiotactic, and atactic polypropylenes synthesized with metallocene catalysts. *Macromolecules* **1998**, *31*, 1335−1340.

(18) Wood-Adams, P. M.; Dealy, J. M.; Groot, A. W. de; Redwine, O. D. Effect of molecular structure on the linear viscoelastic behavior of polyethylene. *Macromolecules* **2000**, *33*, 7489−7499.

(19) Nogales, A.; Hsiao, B. S.; Somani, R. H.; Srinivas, S.; Tsou, A. H.; Balta-Calleja, F. J.; Ezquerra, T. A. Shear-induced crystallization of isotactic polypropylene with different molecular weight distributions: In situ small- and wide-angle X-ray scattering studies. *Polymer* **2001**, *42*, 5247−5256.

(20) Baik, J. J.; Tzoganakis, C. A study of extrudate distortion in controlled-rheology polypropylenes. *Polym. Eng. Sci.* **1998**, *38*, 274−281.

(21) Azizi, H.; Ghasemi, I. Reactive extrusion of polypropylene: production of controlled-rheology polypropylene (CRPP) by peroxide promoted degradation. *Polym. Test.* **2004**, *23*, 137−143.
(22) Sheng, B. R.; Li, B.; Xie, B. H. Influences of molecular weight and crystalline structure on fracture behavior of controlled-rheology-polypropylene prepared by reactive extrusion. *Polym. Degrad. Stab.* **2008**, *93*, 225−232.
(23) Azizi, H.; Ghasemi, I.; Karrabi, M. Controlled-peroxide degradation of polypropylene: Rheological properties and prediction of MWD from rheological data. *Polym. Test.* **2008**, *27*, 548−554.
(24) Bertin, D.; Leblanc, M.; Marque, S. R. A. Polypropylene degradation: Theoretical and experimental investigations. *Polym. Degrad. Stab.* **2010**, *95*, 782−791.
(25) Berzin, F.; Vergnes, B.; Delamare, L. Rheological behavior of controlled-rheology polypropylenes obtained by peroxide-promoted degradation during extrusion: comparison between homopolymer and copolymer. *J. Appl. Polym. Sci.* **2001**, *80*, 1243−1252.
(26) Salazar, A.; Martın, T.; Navarro, J. M. Fracture behaviour of controlled-rheology ethylene−propylene block copolymers. *Polym. Int.* **2011**, *60*, 765−771.
(27) Wang, S. W.; Yang, W.; Xu, Y. J.; Xie, B. H.; Yang, M. B.; Peng, X. F. Crystalline morphology of β-nucleated controlled-rheology polypropylene. *Polym. Test.* **2008**, *27*, 638−644.
(28) Cao, J.; Lv, Q.-F. Crystalline structure, morphology and mechanical properties of β-nucleated controlled-rheology polypropylene random copolymers. *Polym. Test.* **2011**, *30*, 899−906.
(29) Busse, K.; Kressler, J.; Maier, R.; Scherble, J. Tailoring of the α-, β-, and γ-modification in isotactic polypropene and propene/ethene random copolymers. *Macromolecules* **2000**, *33*, 8775−8780.
(30) Yuan, Y.; Chen, B.; Zhang, X. Study on the formation of β-crystal during the crystallization process of polypropylene reactor granule. *Polymer* **2007**, *48*, 5480−5483.
(31) Xua, L.; Xua, K.; Zhang, X.; Liu, F.; Chen, M. The mechanism for fracture resistance in β-nucleated isotactic polypropylene. *Polym. Adv. Technol.* **2010**, *21*, 807−816.
(32) Somani, R. H.; Hsiao, B. S.; Nogales, A.; Fruitwala, H.; Srinivas, S.; Tsou, A. H. Structure development during shear flow induced crystallization of i-PP: In situ wide-angle X-ray diffraction study. *Macromolecules* **2001**, *34*, 5902−5909.
(33) Turner-Jones, A.; Aizlewood, J. M.; Beckett, D. R. Crystalline forms of isotactic polypropylene. *Makromol. Chem.* **1964**, *75*, 134−158.
(34) Li, J. X.; Cheung, W. L.; Jia, D. A study on the heat of fusion of β-polypropylene. *Polymer* **1999**, *40*, 1219−1222.
(35) Li, J. X.; Cheung, W. L. On the deformation mechanisms of β-polypropylene: 1. Effect of necking on β-phase PP crystals. *Polymer* **1998**, *39*, 6935−6940.
(36) Shangguan, Y.; Song, Y.; Peng, M.; Li, B.; Zheng, Q. Formation of β-crystal from nonisothermal crystallization of compression-molded isotactic polypropylene melt. *Eur. Polym. J.* **2005**, *41*, 1766−1771.
(37) Xiao, W. C.; Wu, P. Y.; Feng, J. C. Effect of β-nucleating agents on crystallization and melting behavior of isotactic polypropylene. *J. Appl. Polym. Sci.* **2008**, *108*, 3370−3379.
(38) Arnal, M. L.; Balsamo, V.; Ronca, G.; Sánchez, A.; Müller, A. J.; Cañizales, E.; Urbina de Navarro, C. Applications of successive self-nucleation and annealing (SSA) to polymer characterization. *J. Therm. Anal. Calorim.* **2000**, *59*, 451−470.
(39) Wood-Adams, P. M.; Dealy, J. M.; de Groot, A. W.; Redwine, O. D. Effect of Molecular Structure on the Linear Viscoelastic Behavior of Polyethylene. *Macromolecules* **2000**, *33*, 7489−7499.
(40) Coulon, G.; Castelein, G.; G'Sell, C. Scanning force microscopic investigation of plasticity and damage mechanisms in polypropylene spherulites under simple shear. *Polymer* **1999**, *40*, 95−110.
(41) Henning, S.; Adhikari, R.; Michler, G. H.; Balta-Calleja, F. J.; Karger-Kocsis, J. Micromechanical mechanisms for toughness enhancement in β-modified polypropylene. *Macromol. Symp.* **2004**, *214*, 157−171.
(42) Zhang, P. Y.; Liu, X. X.; Li, Y. Q. Influence of β-nucleating agent on the mechanics and crystallization characteristics of polypropylene. *Mater. Sci. Eng., A* **2006**, *43*, 4310−4313.
(43) Varma-Nair, M.; Agarwal, P. K. Quiesent crystallization kinetics of nucleated metallocene and ZN isotactic polypropylenes. *J. Therm. Anal. Calorim.* **2000**, *59*, 483−495.
(44) Bai, H.; Wang, Y.; Liu, L.; Zhang, J.; Ha, L. Nonisothermal crystallizat ion behaviors of polypropylene with α/β nucleating agents. *J. Polym. Sci., Part B: Polym. Phys.* **2008**, *46*, 1853−1867.
(45) Muller, A. J.; Hernandez, Z. H.; Arnal, M. L.; Sanchez, J. J. Successive self-nucleation/annealing (SSA): A novel technique to study molecular segregation during crystallization. *Polym. Bull.* **1997**, *39*, 465−472.
(46) Kamfjorda, T.; Stori, Aa. Selective functionalization of the ethylene rich phase of a heterophasic polypropylene. *Polymer* **2001**, *42*, 2767−2775.
(47) Kruczala, K.; Bokria, J. G.; Schlick, S. Thermal aging of heterophasic propylene-ethylene copolymers: spatial and temporal aspects of degradation based on ESR, ESR imaging, and FTIR. *Macromolecules* **2003**, *36*, 1909−1919.